# FUT2 promotes the tumorigenicity and metastasis of colorectal cancer cells via the Wnt/β-catenin pathway

PENG LIU[1-3*], JINGYU LIU[1,2*], MENGYANG DING[1,2*], YIJING LIU[1,2], YUE ZHANG[1,2], XIAOMING CHEN[1,2] and ZHENXU ZHOU[4]

[1]Institute of Glycobiological Engineering and [2]Zhejiang Provincial Key Laboratory of Medical Genetics, Key Laboratory of Laboratory Medicine, Ministry of Education, School of Laboratory Medicine and Life Sciences, Wenzhou Medical University, Wenzhou, Zhejiang 325035; [3]Department of Clinical Laboratory, Northwest Women's and Children's Hospital, Xi'an, Shaanxi 710061; [4]Department of Hernia and Abdominal Wall Surgery, The First Affiliated Hospital of Wenzhou Medical University, Wenzhou, Zhejiang 325000, P.R. China

Received July 15, 2022; Accepted January 9, 2023

DOI: 10.3892/ijo.2023.5483

**Abstract.** The incidence of colorectal cancer (CRC), a leading cause of cancer-related mortality, has increased globally. Fucosyltransferase 2 (FUT2), catalyzing the α1, 2-linked fucose in mammals, has been reported to be overexpressed in several malignant cancers, including CRC. However, the effects of FUT2 on CRC remain largely unknown. Herein, it was determined that the FUT2 expression levels in CRC tissues were higher than those in adjacent non-tumor tissues, whereas no association with tumor stage was revealed. The results of biological functional analysis revealed that FUT2 knockdown inhibited the proliferation, migration and invasion of human CRC cells. Moreover, the knockdown of FUT2 arrested the CRC cells at the G0/G1 phase and promoted the apoptosis of human CRC cells. Western blot analysis demonstrated that the expression levels of β-catenin, C-myc and cyclin D1 were decreased by FUT2 knockdown in CRC cells, whereas the expression of glycogen synthase kinase-3β and the phosphorylation levels of β-catenin were increased. Additionally, Wnt2 was fucosylated by FUT2 in CRC cells. Furthermore, the knockdown of FUT2 inhibited the growth of human CRC *in vivo*. Overall, the findings of the present study suggest that FUT2 may be used as a potential diagnostic biomarker and therapeutic target for CRC treatment.

*Correspondence to:* Professor Xiaoming Chen, Institute of Glycobiological Engineering, Key Laboratory of Laboratory Medicine, Ministry of Education, School of Laboratory Medicine and Life Sciences, Wenzhou Medical University, 268 West Xueyuan Road, Wenzhou, Zhejiang 325035, P.R. China
E-mail: xmc@wmu.edu.cn

Dr Zhenxu Zhou, Department of Hernia and Abdominal Wall Surgery, The First Affiliated Hospital of Wenzhou Medical University, 2 Fuxue Lane, Wenzhou, Zhejiang 325000, P.R. China
E-mail: doctorzhouzhenxu@163.com

*Contributed equally

*Key words:* fucosyltransferase 2, proliferation, metastasis, Wnt/β-catenin pathway, colorectal cancer

## Introduction

Colorectal cancer (CRC) is the second leading cause of cancer-related mortality and was the third most commonly diagnosed tumor in 2020, according to global cancer statistics (1,2). The incidence and mortality associated with colorectal cancer are rapidly increasing, due to environmental factors, dietary changes, the aging population and germline genetics (3,4). The incidence of CRC has been increasing in recent years, and the mortality rates of male and female patients with CRC in China have increased (5). Therapies for CRC have notably improved; however, the 5-year survival rate of patients with metastatic CRC remains extremely low, and metastatic CRC, in most cases, remains an incurable disease (6). It is thus imperative to exploit new targets which play crucial roles in carcinogenesis. A more in-depth understanding the underlying molecular mechanisms may prove to be helpful for the exploration of novel diagnostic or potential therapeutic targets for CRC.

Glycosylation, the major post-translational modification of proteins, regulates a number of biological processes including cell proliferation, differentiation, intracellular and intercellular signaling, cell-to-cell communications and immune recognition (7-9). Increasing evidence has revealed that aberrant glycosylation plays crucial roles in tumor proliferation, metastasis, angiogenesis and immune surveillance, and has been cited as a hallmark of cancer (10,11). Aberrant glycosylation can stem from the altered expression of glycosyltransferases, the dysfunction of glycosyltransferases, donor substrate availability, metabolic alterations, and modified molecular chaperone activity (12). Fucosylation, performed by fucosyltransferase, is one of the terminal and important modifications of glycan (13). The aberrant expression of fucosyltransferases (FUTs) has been reported in numerous cancer types and

plays vital biological roles in tumor development (14). The overexpression of FUT7 has been shown to promote A549 cell proliferation by activating the EGFR/AKT/mTOR signaling pathway (15). The high expression of FUT4 has been found to be associated with programmed death-1, immune response and poor overall survival in operable lung adenocarcinoma (LUAD) (16). Another study demonstrated that fucosylation induced by FUT8 was increased in aggressive prostate cancer cells (17). FUT2 catalyzes fucose in the α-1,2-linkage at the terminal of glycan; it is also overexpressed in several cancer types and has been associated with tumor progression. FUT2 is overexpressed in LUAD and promotes LUAD metastasis through the epithelial-mesenchymal transition initiated by TGF-β/Smad signaling (18). FUT1 and FUT2 play crucial roles in the regulation of the tumorigenesis, metastasis and cancer stem cell properties of breast cancer (19). However, the biological role and molecular mechanisms of action of FUT2 in CRC remain unknown.

The Wnt signaling pathway plays crucial roles in cell proliferation, migration and has also been shown to be tightly associated with cancer. The Wnt/β-catenin pathway, also known as canonical Wnt signaling, is crucial for intestinal development and stem cell renewal, and aberrant Wnt/β-catenin signaling is an early event in CRC development, which has most prominently been described in CRC (20,21). In recent years, novel insight into the Wnt/β-catenin pathway was obtained, further clarifying the regulatory mechanisms of the pathway (21).

In the present study, the effects of FUT2 on CRC cell proliferation and metastasis were investigated. FUT2 was overexpressed in CRC tissues and cell lines. The knockdown of FUT2 induced G0/G1 cell cycle arrest and inhibited proliferation, migration and invasion, while promoting the apoptosis of CRC cells. Furthermore, FUT2 regulated the proliferation and metastasis of CRC cells via the Wnt/β-catenin pathway. The findings of the present study revealed the effects of FUT2 in CRC progression, and may thus provide a potential treatment strategy for CRC.

## Materials and methods

*Bioinformatics analysis*. Gene Expression Profiling Interactive Analysis (GEPIA), an online software (http://gepia.cancer-pku.cn) for cancer and normal gene expression profiling and interactive analysis (22), was used to analyze the gene expression levels of FUT2 in colon adenocarcinoma (COAD) and rectal adenocarcinoma (READ). CRC-related data were extracted from The Cancer Genome Atlas (TCGA) database. In total, 275 CAOD tumor samples and 349 normal samples, and 92 READ tumor samples and 318 normal samples were selected and analyzed.

*CRC specimens*. The CRC tissues and their paired adjacent non-cancerous tissues (28 pairs of tissues; median age of patients, 66.4 years; range, 48-89 years) used in the experiments were collected from the First Affiliated Hospital of Wenzhou Medical University between April, 2018 to September, 2018. All cases were from patients diagnosed with CRC and had not received any treatment prior to surgery. The present study was approved by the Ethics Committee of the First Affiliated Hospital of Wenzhou Medical University (Issuing no. 2019-086). CRC tissue microarrays were obtained from Alenabio; Taibsbio (http://www.taibsbio.com/), containing 36 pairs of CRC tissues and adjacent non-tumor tissues, 9 pairs of colorectal cancer lymph node metastatic tissues and normal lymph node tissues, and 8 normal colon tissues and 2 normal rectal tissues (DCO1002c). Clinical staging was based on the International Union for cancer control/American Joint Committee on Cancer (UICC/AJCC) TNM classification (7th edition) (23). Written informed consent was obtained from all participants prior to the commencement of the study.

*Cell lines and cell culture*. The human colorectal cancer cell lines, SW-480 (TCHu172), DLD-1 (TCHu134), HCT-116 (TCHu 99) and HCT-8 (TCHu 18), and the human normal colorectal epithelial cell (FHC; CRL-1831) were obtained from the Cell Bank of the Chinese Academy of Sciences (Shanghai, China). The cells were maintained in DMEM (Gibco; Thermo Fisher Scientific, Inc.) with 10% FBS (fetal bovine serum) (Gibco; Thermo Fisher Scientific, Inc.). All cells were cultured in 37˚C in a 5% $CO_2$ incubator.

*Cell transfection*. The knockdown of FUT2 was achieved with short hairpin RNA (shRNA)-mediated gene silencing using constructed plasmids containing hairpin FUT2 shRNA sequence (sh-FUT2#1: 5'-GGTCAGTTAATTTAG CGGCTC-3', sh-FUT2#2: 5'-GGTAGGAATTGTCACATA CCC-3', sh-NC: 5'-GCTTCGCGCCGTAGTCTTA-3'). For transfection, the 2.5 $\mu$g vectors (pGPU6/GFP/Neo-FUT2 or pGPU6/GFP/Neo-shNC) (GeneCopoeia, Inc.) were transfected into the SW-480 and DLD-1 cells using Lipofectamine 3000 reagent (Invitrogen; Thermo Fisher Scientific, Inc.), with incubation for 15 min at room temperature, according to the manufacturer's instructions. The cells were cultured in DMEM containing 10% FBS and 350 ng/ml puromycin (Beijing Solarbio Science & Technology Co., Ltd.) under 5% $CO_2$ at 37˚C for 2 weeks. The positive clones were verified by using reverse transcription-quantitative PCR (RT-qPCR) and western blot analysis, and used in subsequent experiments.

*siRNA transfection*. For the knockdown of β-catenin, the SW-480 cells [the cells transfected with shFUT2#1 and the respective control (NC); $5x10^5$] were cultured in six-well plates to 60% confluency in DMEM at 37˚C and transfected with 100 pmol/$\mu$l siRNA mixed with Lipofectamine 3000 reagent, and incubated for 15 min at room temperature, according to the manufacturer's instructions (Shanghai GenePharma Co., Ltd.). The siRNA sequences were as follows: siRNA for β-catenin (si-β-catenin), 5'-GAATGCCGTTCGCCTTCA TTA-3'; siRNA for negative control (siNC), 5'-UUCUCCGAA CGUGUCACGUTT-3', (Shanghai GenePharma Co., Ltd.). The cells were incubated at 37˚C for 48 h.

*RT-qPCR*. Total RNA was extracted from the SW-480 or DLD-1 cells using the RNA prep Pure Cell kit (Invitrogen; Thermo Fisher Scientific, Inc.), according to the manufacturer's protocol. cDNA was obtained by reverse transcription using the Prime Script RT reagent kit (RR047A; Takara Bio, Inc.) The reaction conditions were as follows: 37˚C for 15 min

Table I. Primer sequences used for gene expression analysis.

| Gene | Forward (5'-3') | Reverse (5'-3') |
|---|---|---|
| FUT2 | GTGGTGTTTGCTGGCGATGG | AAAGATTTTGAGGAAAGGGGAGTCG |
| GAPDH | GAACATCATCCCTGCCTCTACT | CCTGCTTCACCACCTTCTTG |

FUT2, fucosyltransferase 2.

and 85˚C for 5 sec. The obtained cDNA was quantified using the SYBR® Premix Ex Taq™ (Perfect Real Time) qPCR kit (Takara Bio, Inc.), and detected using an ABI real-time fluorescent quantitative PCR system (Applied Biosystems; Thermo Fisher Scientific, Inc.). The PCR was performed as follows: 95˚C for 3 min, followed by 40 cycles of denaturation at 95˚C for 10 sec and annealing at 60˚C for 30 sec. The primers used for RT-qPCR are listed in Table I. The $2^{-\Delta\Delta Cq}$ method was used to calculate the difference in gene expression, and GAPDH was used as the internal reference gene (24).

*Cell proliferation assay*. The Cell Counting Kit-8 (CCK-8) was used to measure cell viability. In brief, the cells were incubated in 96-well plates at a density of 5,000 cells/well at 37˚C with 5% $CO_2$. Following cell culture for 24, 48, or 72 h, the cells were washed with PBS, and 10 $\mu$l CCK-8 reagent (Dojindo Laboratories, Inc.) was added to each well. The samples were measured using an automatic ELISA plate reader (Varioskan Flash; Thermo Fisher Scientific, Inc.) at a wavelength of 450 nm.

*Colony formation assay*. For colony formation assay, the SW-480 and DLD-1 cells were digested, resuspended in complete DMEM and seeded in six-well plates (500 cells/well) containing 2 ml DMEM. Following incubation at 37˚C for 2 weeks, the cells were fixed with 4% paraformaldehyde for 20 min, then stained with 0.1% crystal violet (Beyotime Institute of Biotechnology) at room temperature for 30 min. Images were obtained under a microscope (TS100; Nikon Corporation), and colonies were counted and analyzed using Image J software (v1.8.0; National Institutes of Health).

*Wound healing assay*. SW-480 and DLD-1 cells were seeded in six-well plates with a density of $1x10^6$ cells/well. Following cell culture up to 80-90% confluency in 10% serum, the cells were scratched to form two parallel straining lines, and non-adherent cells were washed off with PBS. Images of the wounds were photographed under a microscope (TS100; Nikon Corporation) at 0 and 48 h, respectively, and the wound widths were calculated using Image J software (v1.8.0; National Institutes of Health). Values were calculated by applying the following formula: Percentage of wound closure=1-($width_t$/$width_0$).

*Transwell migration and invasion assays*. Transwell chambers (24-well; Corning, Inc.) were used to assess the migratory and invasive ability of the CRC cells (SW-480 and DLD-1). For the migration assay, cells ($6x10^4$ cells/well) were re-suspended in serum-free DMEM and seeded into the upper chamber with an 8 $\mu$m pore size, and into the lower chamber, DMEM with 10% FBS was added. Following cell culture for 24 h at 37˚C, the chambers were washed with PBS. Subsequently, the cells that had migrated to the lower chamber were fixed with 4% paraformaldehyde at room temperature for 30 min, then stained with crystal violet (Beyotime Institute of Biotechnology) at room temperature for 30 min. Finally, images were captured under a microscope (TS100; Nikon Corporation) and the numbers of cells were counted.

For the invasion assays, the experimental procedure applied was similar to that described above for migration, with the difference that the upper chamber was pre-coated with BD Matrigel (BD Biosciences) at 37˚C for 8 h according to the manufacture's protocol for the invasion assay, and cells were cultured for 48 h.

*Flow cytometry*. Flow cytometry was used to assess the cell cycle and apoptosis. For the cell cycle assay, SW-480 and DLD-1 cells ($1x10^6$ cells/well) were seeded in six-well plates in DMEM with 10% FBS and cultured for 48 h. Following trypsinization and washing with PBS, cells were fixed in 70% ethanol at 4˚C for 2 h. Subsequently, the samples were resuspended in the staining buffer with propidium iodide (PI; Nanjing KeyGen Biotech Co., Ltd.) and RNase A (the ratio of PI to RNase A was 9:1), and incubated in the dark for 30 min at room temperature. Finally, the samples were analyzed using a flow cytometer (FACS Arial, BD Biosciences). The proportion of cells in the S + G2 phase was calculated using FlowJo v10.8.1 software (BD Biosciences).

For the apoptosis assay, the cells were harvested and incubated with Annexin V-APC and PI using an Annexin V-APC/PI Apoptosis Detection kit (Bio-Rad Laboratories, Inc.), according to the manufacturer's instructions, and analyzed using a flow cytometer (as described above).

*Western blot analysis*. The processed cells (SW-480, DLD-1, HCT-116, HCT-8 and FHC) and tissues were lysed in RIPA buffer (Beyotime Institute of Biotechnology) supplemented with 0.1% protease inhibitors (MilliporeSigma), and proteins were obtained according to the manufacturer's protocol. The supernatant was collected by centrifugation (20,900 x g, 30 min, 4˚C). The protein concentration was measured using a BCA Protein Assay kit (Beyotime Institute of Biotechnology). For western blot analysis, the extracted protein (20 $\mu$g) was separated by 10% sodium dodecyl sulfate-polyacrylamide gel electrophoresis (SDS-PAGE), and electro-transferred onto polyvinylidene fluoride (PVDF) membranes (MilliporeSigma). The membranes were blocked with 5% non-fat milk in Tris buffer saline with 0.1% Tween-20 (TBST) at room temperature for 2 h, and subsequently incubated with specific primary antibodies at 4˚C overnight. After washing with TBST, the

membranes were incubated with the corresponding secondary antibodies at room temperature for 1 h, and visualized using an enhanced chemiluminescence (ECL) reagent (NCM USA). The results were analyzed using Image J software (v1.8.0; National Institutes of Health). The primary antibodies used were as follows: FUT2 (cat. no. sc-100742) was obtained from Santa Cruz Biotechnology, Inc. Antibodies against C-myc (ab32072), cyclin D1 (ab134175) and phosphorylated (p-) β-catenin (cat. no. ab47335) were purchased from Abcam. Primary antibody against glycogen synthase kinase-3β (GSK3β; cat. no. 12456) was acquired from Cell Signaling Technology, Inc. Primary antibodies against β-catenin (51067-2-AP), and Wnt2 (66656-1-Ig) were obtained from Proteintech Group, Inc. Antibodies against tubulin (db3285), GAPDH (db1209) and β-actin (db10001) were purchased from Diagbio (http://www.daigebio.com), and used as the loading controls. HRP-conjugated Affinipure goat anti-rat IgG (A0206) and HRP-conjugated Affinipure goat anti-rabbit IgG (A0208) were used as the secondary antibodies and purchased from Beyotime Institute of Biotechnology.

*Immunohistochemistry (IHC)*. The paraffin-embedded tissue sections (5-$\mu$m-thick) were purchased from Alenabio; Taibsbio (http://www.taibsbio.com/). For IHC staining, the tissue sections were used as previously described (25). Briefly, the tissues were deparaffinized with xylene, rehydrated with ethanol, followed by antigen retrieval with sodium citrate solution and endogenous peroxidase blocking with 3% $H_2O_2$ at room temperature for 30 min. Following blocking with 5% bovine serum albumin (BSA; Beyotime Institute of Biotechnology), the samples were incubated with an antibody against FUT2 (ab177239; 1:150; Abcam) at 4˚C overnight, and were subsequently incubated with biotinylated secondary antibodies (enhancement of enzyme-labeled goat anti-rabbit IgG; A0279; Beyotime Institute of Biotechnology) for 1 h at room temperature, treated with 3,3'-diaminobenzidine (D12384; Merck KGaA), and finally counterstained with hematoxylin (C0105S; Beyotime Institute of Biotechnology) at room temperature for 3 min. Images were obtained using a microscope (TS100; Nikon Corporation).

*Immunofluorescence*. The immunofluorescence assays were performed as previously described (26). Briefly, the processed cells were washed with PBS three times, and fixed with 4% paraformaldehyde at room temperature for 30 min. After washing with PBS, the cells were permeabilized with 0.5% Triton X-100 for 15 min at room temperature, and then blocked with 5% BSA for 2 h at room temperature. Subsequently, the cells were incubated with an anti-β-catenin antibody (51067-2-AP; Thermo Fisher Scientific, Inc.) at 4˚C overnight, then incubated with the secondary antibody Cy3-conjugated anti-rabbit antibody (A0516; Beyotime Institute of Biotechnology) in the dark for 1 h at room temperature, stained with 0.5 $\mu$g/ml DAPI (4',6-diamidino-2-phenylindole) (MilliporeSigma) at room temperature for 10 min to dye the nucleus. The samples were analyzed using a confocal laser scanning microscope (Nikon Corporation).

*Co-immunoprecipitation*. The SW-480 cells ($5x10^6$ cells) were lysed using RIPA buffer as mentioned above. The cell lysate was centrifuged at 20,900 x g for 20 min at 4˚C. The cell lysate was pre-cleared using sepharose-protein A/G beads (ab193262; Abcam) 4˚C for 2 h, and IgG was used as a control. The supernatant was collected and incubated with primary antibody (Wnt2, 66656-1-Ig, 1:1,000, Thermo Fisher Scientific, Inc.; FUT2, sc-100742, 1:200, Santa Cruz Biotechnology) at 4˚C overnight, and sepharose-protein A/G beads were then added and incubated at 4˚C for 2 h. The protein-antibody complexes were collected and resuspended in the SDS buffer. Finally, the samples were boiled at 100˚C for 10 min, the magnetic beads were removed, and the binding proteins were obtained for western blot analysis as described above.

*Lectin pull-down*. The SW-480 cells ($5x10^6$ cells) were lysed using RIPA buffer as mentioned above. Cell lysates ere incubated with Agarose-bound (Ulex Europaeus Agglutin-1 (UEA-1; AL-1063; Vector Laboratories, Inc.) and rotated overnight at 4˚C. After washing, the precipitated proteins were further examined using western blot analysis with Wnt2 antibody. The BCA Protein Assay kit was used to measure the protein concentration.

*Xenograft nude mouse model*. BALB/c nude mice (12 females, 4 to 5 weeks old, weighing 20-22 g) were purchased from the Beijing Vital River Laboratory Animal Technology Co., Ltd. The mice were housed at ~25˚C and 50% humidity with a 12/12-h light/dark cycle, and *ad libitum* access to food and water. For the *in vivo* subcutaneous tumorigenesis assay, shNC or shFUT2 SW-480 cells (50 $\mu$l, $2x10^7$ cells/ml in DMEM) were mixed with 50 $\mu$l 50% BD Matrigel and injected into the subcutaneous right flanks of the BALB/C-nu nude mice (six mice per group). Animal health and behavior was observed every 2 days throughout the study period, and the tumors were measured every week. No mice died during the experiment. Human endpoints were reached when the maximum tumor volume was >750 $mm^3$. After 30 days, a total of 12 mice (six per group) were anesthetized using 2% pentobarbital sodium (60 mg/kg, intraperitoneal injection) followed by cervical dislocation. The death of all experimental animals was verified though the cessation of respiration, heartbeat and nerve reflex. Subsequently, the tumors were collected, weighed and measured. Tumor volume ($mm^3$) was calculated using the following formula: Volume=0.5 x length x $width^2$. The animal experiment was approved by the Laboratory Animal Ethics Committee of Wenzhou Medical University and Laboratory Animal Centre of Wenzhou Medical University (reference no. WYDW2019-0245).

*Statistical analysis*. Comparisons between two groups were performed using an unpaired Student's t-test or one-way ANOVA analysis followed by Tukey's test. Statistical analyses were performed using SPSS software version 17.0 (SPSS, Inc.). Data are expressed as the mean ± SD of at least three repeated experiments. $P<0.05$ was considered to indicate a statistically significant difference.

## Results

*FUT2 expression is upregulated in CRC*. GEPIA was used in order to analyze the expression levels of FUT2 in CRC. As

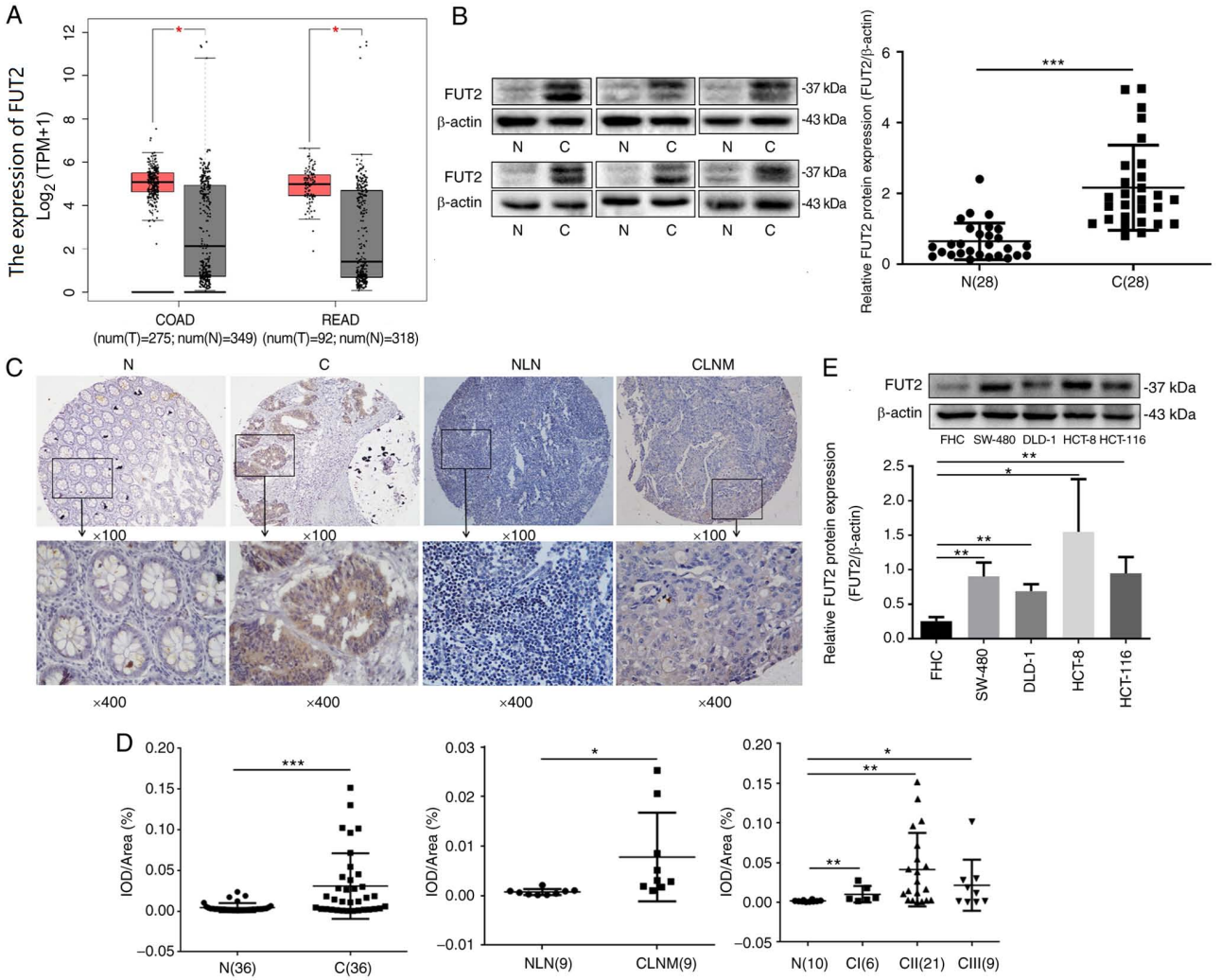


Figure 1. FUT2 is overexpressed in colorectal cancer tissues and cell lines. (A) Boxplot illustrating the relative expression of FUT2 in normal, COAD and READ samples. (B) Evaluation of FUT2 expression in fresh human colorectal cancer tissues and adjacent normal tissues using western blot analysis. C, colorectal cancer tissues; N, normal tissues. (C) Representative images of the expression of FUT2 proteins assessed using immunohistochemistry. C1, colorectal cancer tissues; N1, adjacent tissues; CLNM, colorectal cancer lymph node metastatic tissue; NLN, normal lymph node tissue. Magnification: Upper panels, x100; lower panels, x400. (D) Quantitative analysis of the average MOD of FUT2 staining in normal tissues, colorectal cancer tissues and lymph node metastatic tissues. N, normal control; CI, cancer stage I; CII, cancer stage II; CIII, cancer stage III. (E) The expression of FUT2 in colorectal cancer cell lines and FHC was examined using western blot analysis. β-actin was used as the loading control. Data are expressed as the mean ± SD. $^{*}$P<0.05, $^{**}$P<0.01 and $^{***}$P<0.001. FUT2, fucosyltransferase 2; COAD, colon adenocarcinoma; READ, rectal adenocarcinoma; MOD, mean optical density.

demonstrated in Fig. 1A, the expression of FUT2 was upregulated both in COAD (n=275) and READ (n=92), as compared with normal colorectal tissue (n=349, n=318, respectively). To further determine the expression of FUT2 in CRC, the FUT2 protein levels were detected using western blot analysis in CRC tissues and matched tumor-adjacent tissues (n=28). The expression of FUT2 was found to be significantly increased in CRC tissues, compared with the adjacent non-cancerous tissue (Fig. 1B). The observed double bands for FUT2 may be the outcome of FUT2 modification or degradation. FUT2 was also evaluated using IHC in 36 pairs of CRC tissues and adjacent non-cancerous tissues, and nine pairs of CRC lymph node metastatic tissues and the normal lymph node tissues (Fig. 1C). As shown in Fig. 1D, the expression of FUT2 in CRC tissues was significantly increased, compared with the adjacent non-cancerous tissues. The expression of FUT2 in colorectal cancer lymph node metastatic tissues was also increased, compared with the normal lymph node tissues. In order to further evaluate the clinical significance of FUT2, FUT2 expression in the different stages of CRC was analyzed. Compared to normal colon and rectal tissues, the expression of FUT2 was increased in stage I, II and III CRC tissues. However, there was no significant difference among the stage I, II and III (P>0.05, ANOVA with Tukey's post hoc test) samples (Fig. 1D), indicating that the FUT2 level was not associated with the TNM stage. Furthermore, FUT2 expression was detected in SW-480, DLD-1, HCT-116, HCT-8 and FHC cells. As demonstrated in Fig. 1E, FUT2 protein expression in CRC cells (SW-480, DLD-1 and HCT-116) was higher than that in FHC cells. Overall, these results suggested that the upregulation of FUT2 may be associated with CRC development and progression.

*Knockdown of FUT2 suppresses the migration and invasion of CRC cells*. To detect the effects of FUT2 on CRC progression *in vitro*, the SW-480 and DLD-1 cell lines were selected

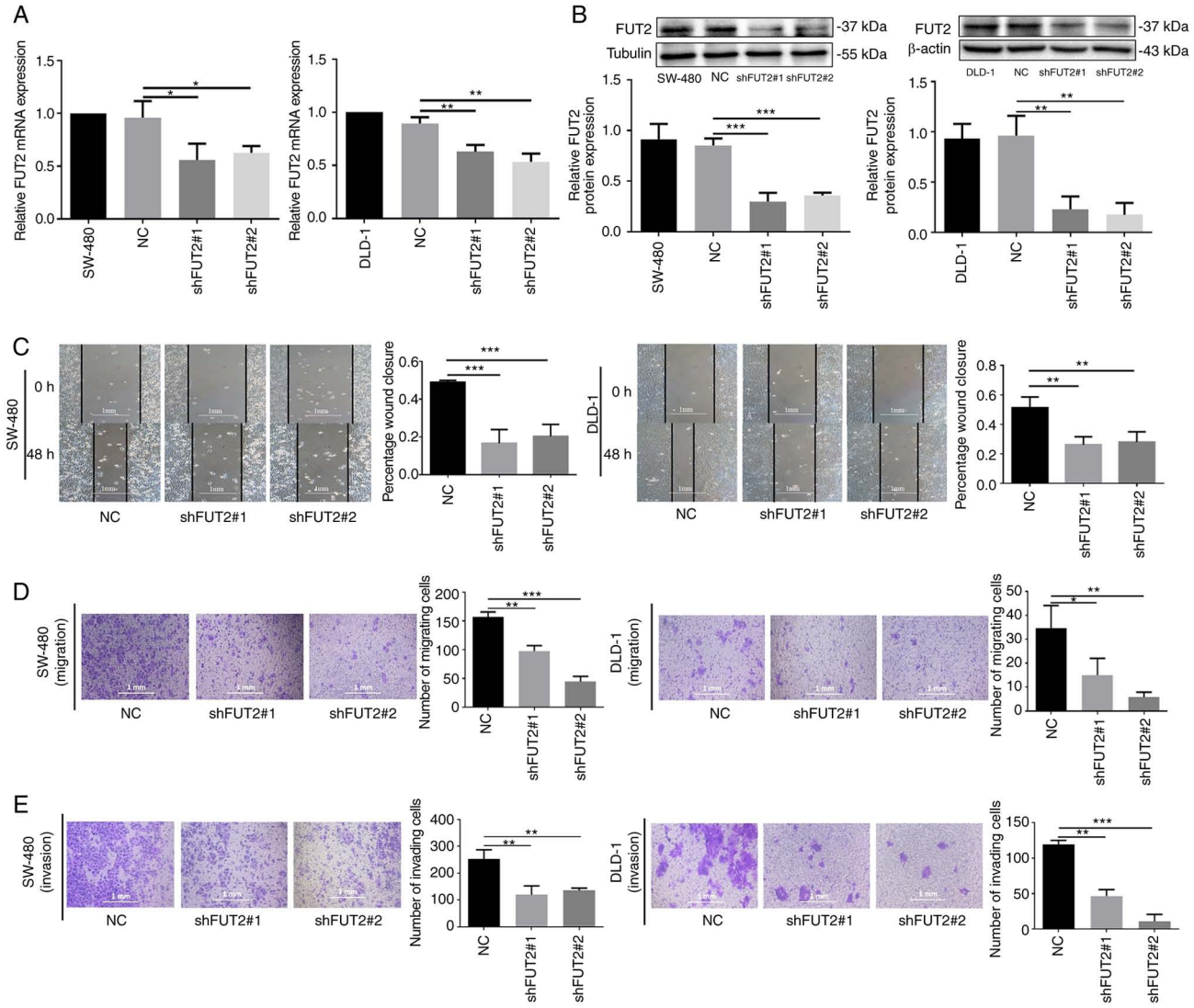


Figure 2. Effects of FUT2 on the migration and invasion of colorectal cancer cells. (A) The mRNA and (B) protein expression of FUT2 was examined using reverse transcription-quantitative PCR and western blot analysis, respectively. (C) The effect of FUT2 on cell migration was measured using a wound healing assay. The migration rates of SW-480 and DLD-1 cells were calculated using the formula described in the 'Materials and methods' section. Scale bar, 1 mm. (D) The effect of FUT2 on cell migration was measured using Transwell assay, and the numbers of migrated cells were calculated. Scale bar, 1 mm. (E) Matrigel invasion assay was performed to assess the invasion of SW-480 and DLD-1 cells, and the numbers of invasive cells were calculated. Scale bar, 1 mm. Data are expressed as the mean ± SD. $^{*}$P<0.05, $^{**}$P<0.01 and $^{***}$P<0.001. FUT2, fucosyltransferase 2.

for further experiments. FUT2-knockdown cells (shFUT2; shFUT2#1 and shFUT2#2) were generated by transfecting the plasmid DNA vector encoding an shRNA that targets FUT2 for the inhibition of FUT2 expression in CRC cell lines (SW-480 and DLD-1), and their corresponding scrambled vector (NC) was used as a control. The mRNA expression levels of FUT2 were markedly decreased in SW-480 cells in which FUT2 was knocked down (shFUT2#1, shFUT2#2), compared with the NC cells, and a similar effect was observed in the DLD-1 cells (Fig. 2A). The results of western blot analysis revealed that the protein levels of FUT2 were also significantly decreased in the shFUT2#1 and shFUT2#2 groups, as compared with the NC group (Fig. 2B).

Wound healing and Transwell assay were then performed to evaluate the effects of FUT2 on cell migration and invasion. As depicted in Fig. 2C, the knockdown of FUT2 significantly inhibited the wound closure, compared with the control cells (NC), suggesting that FUT2 knockdown inhibited the migration of SW-480 and DLD-1 cells. Furthermore, Transwell assay revealed that the number of SW-480 and DLD-1 cells that migrated through the membrane was significantly decreased in the shFUT2 groups (shFUT#1, shFUT2#2), as compared with their corresponding NC group (Fig. 2D). Consistent with results of the wound healing assay, FUT2 knockdown inhibited CRC cell migration. As depicted in Fig. 2E, Matrigel invasion assay revealed that the invasive capacity of the SW-480 and DLD-1 cells was also markedly suppressed in the shFUT2 groups (shFUT#1 and shFUT2#2). These findings suggested that FUT2 promoted the migration and invasion of CRC cells.

*Knockdown of FUT2 inhibits CRC growth in vitro and in vivo.* CCK-8 and plate clone formation assays were then performed in order to determine the role of FUT2 in the growth of CRC cells. The knockdown of FUT2 (shFUT2#1 and shFUT2#2) significantly inhibited the growth of CRC cells (SW-480 and DLD-1), as shown by CCK-8 assay (Fig. 3A). Similarly, the

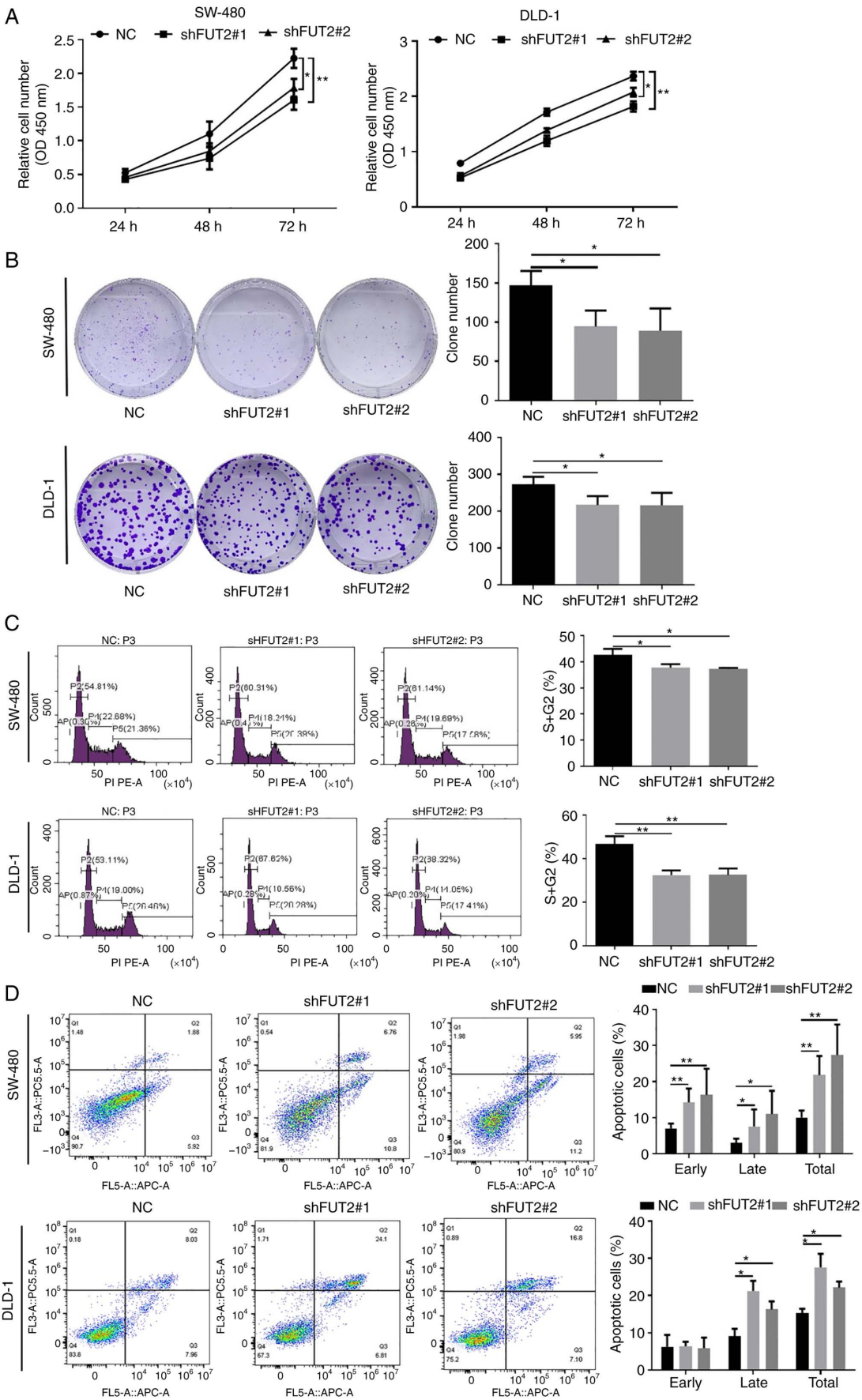


Figure 3. Effects of FUT2 on the proliferation and apoptosis of colorectal cancer cells. (A) The proliferation of SW-480 and DLD-1 cells was measured using CCK-8 assay. (B) The colony-forming ability was determined in the SW-480 and DLD-1 cells. The numbers of colonies were calculated. (C) The cell cycle status of SW-480 and DLD-1 cells was analyzed using flow cytometry. The population cells in the S + G2 phase was calculated. (D) Flow cytometry was performed to analyze the apoptosis of SW-480 and DLD-1 cells. The apoptotic rate of each group was analyzed. Data are expressed as the mean ± SD. $^{*}$P<0.05 and $^{**}$P<0.01. FUT2, fucosyltransferase 2.

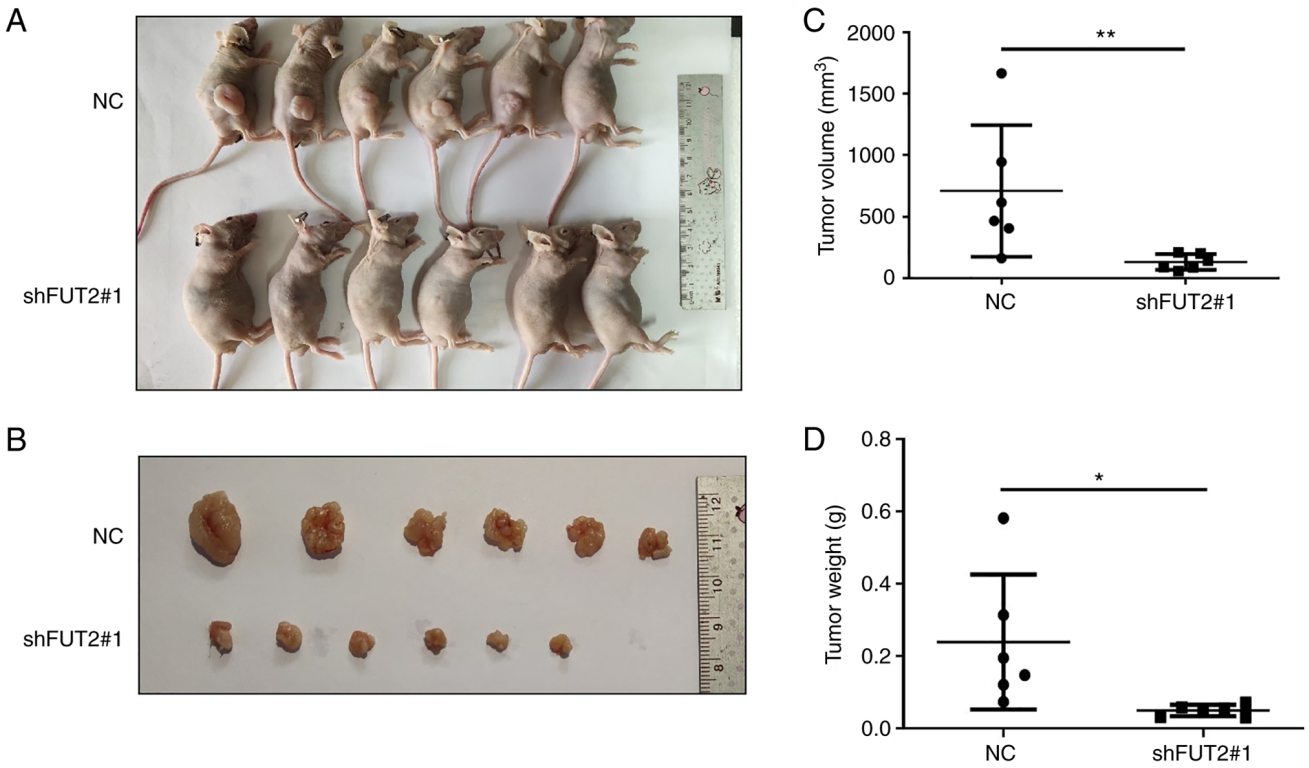


Figure 4. Effects of FUT2 on the growth of SW-480-derived xenograft tumors in nude mice. (A) Images of mice and (B) tumors are presented. (C) The tumor volume of each group was measured and calculated using the formula described in the 'Materials and methods' section. (D) The tumors were weighed. $^{*}$P<0.05 and $^{**}$P<0.01. FUT2, fucosyltransferase 2.

number of cell colonies was markedly decreased in the shFUT2 groups, compared with the NC groups (Fig. 3B). It was thus demonstrated that the knockdown of FUT2 suppressed the proliferation of CRC cells.

To further explore the role of FUT2 in CRC, flow cytometric analysis was used to examine cell cycle progression and apoptosis. The knockdown of FUT2 led to an increase in the cell ratio at the G0/G1 phase, with a marked decrease in the number of cells in the S phase (Fig. 3C), indicating that the CRC cells subjected to FUT2 knockdown were arrested at the G0/G1 phase. Furthermore, the results of flow cytometry demonstrated that the apoptotic indexes were significantly higher in the shFUT2 groups than the NC groups (Fig. 3D), indicating that FUT2 knockdown promoted the apoptosis of CRC cells. On the whole, these results indicated that the knockdown of FUT2 suppressed CRC progression by inhibiting cell proliferation and promoting apoptosis.

To further assess the effects of FUT2 on CRC *in vivo*, a mouse CRC xenograft model was established. As demonstrated in Fig. 4B, the harvested tumors in the shFUT2 group were smaller than the tumors in the NC group. The average lengths of the total number of tumors in the NC and shFUT2 groups were 12.48±3.39 mm and 9.87±2.53 mm, respectively. The average widths of the total number of tumors in the NC and shFUT2 groups were 7.05±1.30 mm and 5.65±0.95 mm, respectively. The average tumor volume of the shFUT2 group was 710.1 $mm^3$, and the average tumor volume of the NC group was 131.4 $mm^3$ (Fig. 4C). The average tumor weight of the NC and shFUT2 groups was 0.239 and 0.050 g, respectively (Fig. 4D). FUT2 knockdown significantly inhibited tumor growth *in vivo*.

*FUT2 promotes CRC progression via β-catenin signaling.* Wnt signaling is tightly associated with cancer and has most prominently been described for CRC (21). In the present study, to elucidate the underlying molecular mechanisms of FUT2 in CRC development, the canonical Wnt/β-catenin signaling was investigated. As depicted in Fig. 5A, the knockdown of FUT2 markedly decreased the expression of β-catenin and increased the phosphorylation of β-catenin (Fig. 5A), which is known to be regulated by GSK3β, and subsequent β-catenin ubiquitination and degradation (27). It was revealed that the expression of GSK3β was significantly increased in the shFUT2 groups, compared with the NC group, which suggested that the knockdown of FUT2 promoted GSK3β expression (Fig. 5B). Moreover, the expression levels of cyclin D1 and C-myc were significantly decreased in the shFUT2 groups (shFUT2#1 and shFUT2#2), as compared with the NC group (Fig. 5C). To further confirm the effects of FUT2 on β-catenin signaling, the distribution of β-catenin was examined using confocal laser microscopy. It was demonstrated that the level of nuclear β-catenin was markedly reduced following FUT2 knockdown (Fig. 5D). Furthermore, the knockdown of β-catenin or FUT2 inhibited the expression of C-myc and cyclin D1, the target genes of β-catenin. The simultaneous knockdown of β-catenin and FUT2 significantly enhanced the suppressive effects of β-catenin or FUT2 knockdown on the expression of C-myc and cyclin D1 in the SW-480 cells (Fig. 5E), suggesting that FUT2 promoted the expression of C-myc and cyclin D1 via β-catenin signaling.

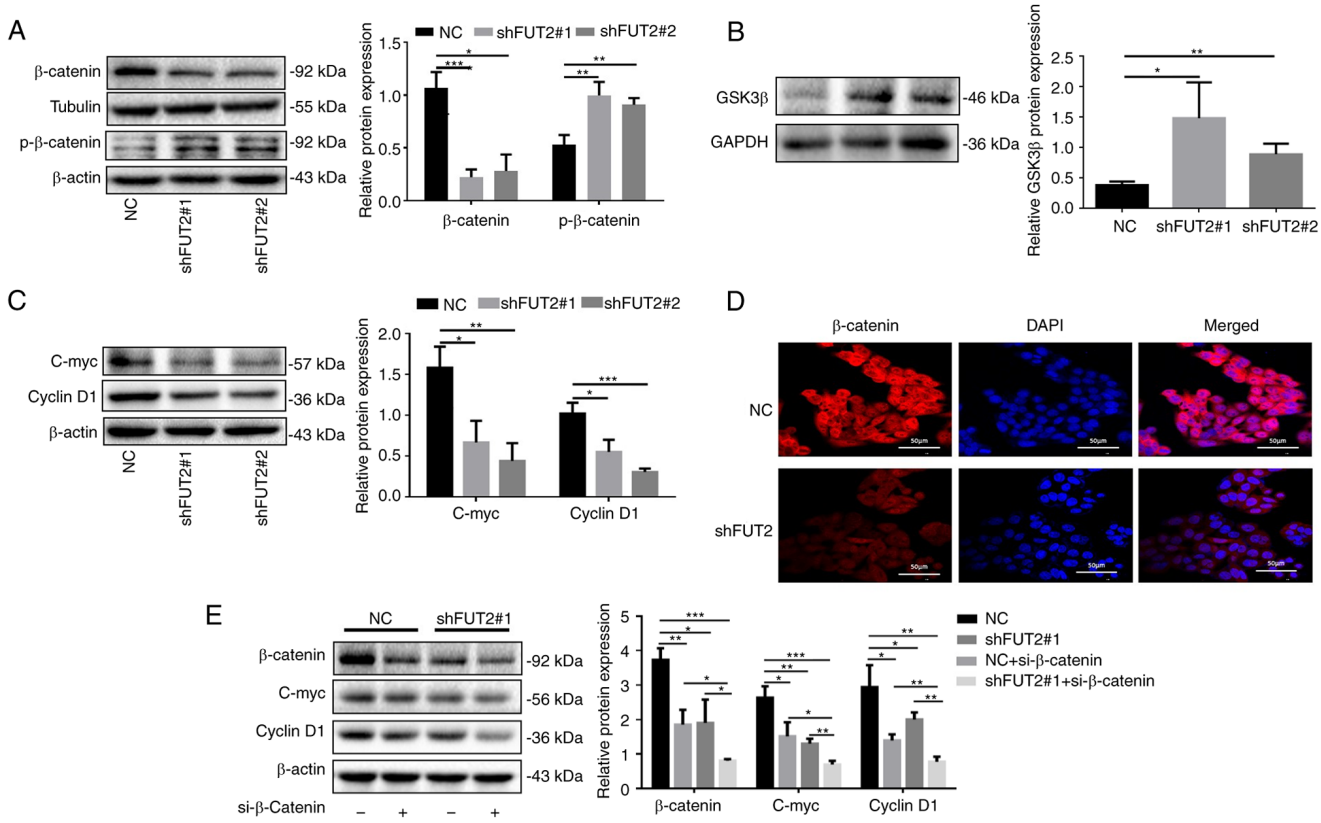


Figure 5. Effects of FUT2 on the Wnt/β-catenin signaling pathway in colorectal cancer cells. (A) The expression of β-catenin and p-β-catenin in SW-480 cells was measured using western blot analsyis. The intensity was evaluated using ImageJ software. The expression of (B) GSK3β, and (C) C-myc and cyclin D1 in SW-480 cells measured using western blot analysis. (D) The distribution of β-catenin in SW-480 cells was measured using immunofluorescent assay. Scale bar, 50 $\mu$m. (E) The expression of β-catenin, C-myc and cyclin D1 in SW-480 cells in which FUT2 or β-catenin was knocked down was measured using western blot analysis. Data are expressed as the mean ± SD. $^{*}$P<0.05, $^{**}$P<0.01 and $^{***}$P<0.001. FUT2, fucosyltransferase 2; GSK3β, glycogen synthase kinase-3β.

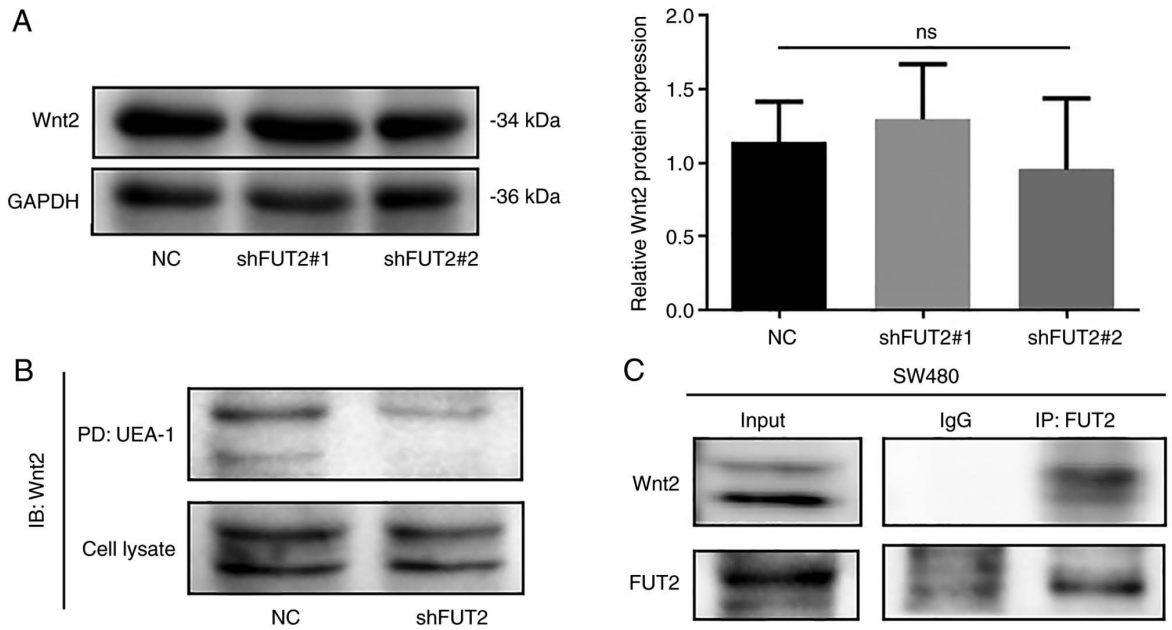


Figure 6. Effects of FUT2 on Wnt2 in colorectal cancer cells. (A) The expression of Wnt2 in SW-480 cells was evaluated using western blot analysis. (B) The α-1,2-fucosylation of Wnt2 was detected by UEA-1 lectin pull-down assay in SW-480 cells. (C) The interaction between FUT2 and Wnt2 was detected using co-immunoprecipitation assay. FUT2, fucosyltransferase 2.

*FUT2 regulates the fucosylation of Wnt2 in CRC cells*. In the canonical Wnt pathway, the phosphorylation and degradation of β-catenin are regulated by Wnt (21). In the present study, to further elucidate the role of FUT2 in the regulation of the

Wnt/β-catenin pathway, lectin pull-down and immunoprecipitation, and western blot analysis were performed. The results of western blot analysis revealed that the protein levels of Wnt2 were not affected by FUT2 knockdown (Fig. 6A). UEA-1 pull-down revealed that the knockdown of FUT2 markedly decreased the fucosylation of Wnt2 (Fig. 6B). Immunoprecipitation and western blot analysis also demonstrated that FUT2 interacted with Wnt2 (Fig. 6C). These results suggested that the FUT2-mediated fucosylation of Wnt2 may activate Wnt/β-catenin signaling.

## Discussion

CRC is a disease of the digestive system and is associated with a high morbidity and mortality, and a poor clinical outcome. Although the clinical treatment of CRC has improved, the prognosis of CRC remains poor. Therefore, it is crucial to elucidate the underlying mechanisms of CRC tumorigenesis and development, in order to improve diagnosis and the treatment effects. Cancer progression has been associated with a variation of protein expression and post-translational modifications (28). Over the past few decades, accumulating evidence has demonstrated that aberrant glycosylation plays a vital role in cancer (29). The alteration of glycosylation may be explained by the dysregulation of glycosyltransferases, which catalyze glycosylation in order to create glycan structures (30,31). Recently, it has been revealed that fucosyl transferases are overexpressed in cancer, including CRC, and mediate several specific biological functions (32,33). Herein, based on TCGA data analysis for FUT2 in CRC, FUT2 expression was analyzed using the GEPIA web-portal. The expression of FUT2 was upregulated in CRC. Furthermore, IHC assay and western blot analysis revealed that the FUT2 protein levels in CRC tissues were increased in comparison with those in adjacent non-cancerous tissues. However, no association with clinical stage was detected. Furthermore, FUT2 was expressed in CRC cells at significantly higher levels than in FHC cells. These results thus suggested that FUT2 may be a positive regulator of the progression of CRC. In the present study, SW-480 and DLD-1 cells were used to investigate the functional role and the molecular mechanisms of FUT2 in CRC.

Functionally, the results of the present study demonstrated that the knockdown of FUT2 attenuated the viability and growth of CRC cells, and inhibited CRC growth *in vivo*. The dysregulation of the cell cycle, as one of the hallmarks of tumor cells, is associate with limitless tumor cell proliferation and growth, and the regulation of cell cycle can be used to prevent cancer development (34). The present study demonstrated that FUT2 knockdown induced the G0/G1 phase arrest of the SW-480 and DLD-1 cells, which may eventually decelerate CRC growth. As a type of programmed cell death, apoptosis is the reverse of cell proliferation and plays a crucial role in maintaining cell and tissue homeostasis (35). In the present study, the knockdown of FUT2 significantly increased the apoptosis of CRC cells. Moreover, FUT2 knockdown inhibited the migratory and invasive capabilities of the SW-480 and DLD-1 cells. These findings suggested that FUT2 may be a positive regulator of CRC development.

The Wnt pathway, a highly conserved and versatile pathway, is critical for cell differentiation, proliferation, tissue homeostasis and regeneration, and is involved in almost all stages of tumor development (36,37). The Wnt pathway is commonly divided into β-catenin-dependent and -independent signaling. Known as 'canonical Wnt signaling', the β-catenin-dependent pathway (Wnt/β-catenin pathway) is considered as the most crucial and well-characterized pathway, and functions by regulating the stabilization and nuclear translocation of β-catenin, thereby regulating cellular processes (38). The stabilization of β-catenin is considered as one of the 'gatekeepers' of Wnt signaling in tumorigenesis (39). Herein, the findings of western blot analysis and confocal laser microscopy revealed that the knockdown of FUT2 reduced the expression of β-catenin, cyclin D1 and C-myc in SW-480 cells, indicating that FUT2 may induce Wnt/β-catenin signaling in CRC cells. The stabilization of β-catenin is determined by its phosphorylation status. When Wnt is inactivated, β-catenin is recruited by APC and delivered to the 'destruction complex', subsequently being degraded following phosphorylation and ubiquitination (40). The results of the present study revealed that the knockdown of FUT2 increased the phosphorylation levels of β-catenin and GSK3β expression, which mediated the phosphorylation of β-catenin. Furthermore, the simultaneous downregulation of FUT2 and β-catenin enhanced the suppressive effect of the sole downregulation of FUT2 on C-myc and cyclin D1 expression. These results indicated that FUT2 promoted CRC cell growth and metastasis via the Wnt/β-catenin pathway.

Among 19 Wnt ligands in mammals, Wnt2, one of the WNT gene family members, is overexpressed in human cancers, including ovarian cancer, lung cancer, pancreatic cancer and CRC (41,42). Wnt2, as a potential marker in CRC, plays tumorigenic roles through the induced activation of β-catenin in CRC (43). In the present study, FUT2 knockdown did not affect the expression of Wnt2; however, the fucosylation of Wnt2 was significantly reduced by FUT2 knockdown, and the interaction between FUT2 and Wnt2 was verified using co-immunoprecipitation/western blot analysis. These results suggested that the FUT2-mediated fucosylation of Wnt2 activated Wnt/β-catenin signaling.

In conclusion, the present study demonstrates that FUT2 is overexpressed in CRC, promoting the tumor growth and metastasis in CRC, and regulating CRC tumorigenesis via the Wnt/β-catenin signaling pathway. These findings may indicate the role of FUT2 as a potential diagnostic or therapeutic target for CRC.

## Acknowledgements

The authors would like to acknowledge the Key Discipline of Zhejiang Province in Medical Technology (First Class, Category A) for their support (which included technology and communication platforms, large scale equipment, training).

## Funding

The present study was supported by the Wenzhou Science and Technology Bureau (grant no. Y20210180).

## Availability of data and materials

The datasets used and/or analyzed during the current study are available from the corresponding author on reasonable request.

## Authors' contributions

XC and ZZ participated in the conceptualization of the study. PL, JL, MD, YL and YZ performed the experiments, data collection and data interpretation. XC and ZZ prepared and revised the manuscript. PL and XC confirm the authenticity of all the raw data. All authors have read and approved the final manuscript.

## Ethics approval and consent to participate

The present study was approved by the Ethics Committee of the First Affiliated Hospital of Wenzhou Medical University (Issuing no. 2019-086). Written informed consent was obtained from all participants prior to the commencement of the study. The animal experiments were approved (reference no. WYDW2019-0245) by the Laboratory Animal Ethics Committee of Wenzhou Medical University and Laboratory Animal Centre of Wenzhou Medical University (Wenzhou, China).

## Patient consent for publication

Not applicable.

## Competing interests

The authors declare that they have no competing interests.

## References


1. Siegel RL, Miller KD, Fuchs HE and Jemal A: Cancer statistics, 2022. CA Cancer J Clin 72: 7-33, 2022.
2. Sung H, Ferlay J, Siegel RL, Laversanne M, Soerjomataram I, Jemal A and Bray F: Global cancer statistics 2020: GLOBOCAN estimates of incidence and mortality worldwide for 36 cancers in 185 countries. CA Cancer J Clin 71: 209-249, 2021.
3. Akimoto N, Ugai T, Zhong R, Hamada T, Fujiyoshi K, Giannakis M, Wu K, Cao Y, Ng K and Ogino S: Rising incidence of early-onset colorectal cancer-a call to action. Nat Rev Clin Oncol 18: 230-243, 2021.
4. Pandurangan AK, Divya T, Kumar K, Dineshbabu V, Velavan B and Sudhandiran G: Colorectal carcinogenesis: Insights into the cell death and signal transduction pathways: A review. World J Gastrointest Oncol 10: 244-259, 2018.
5. Xia C, Dong X, Li H, Cao M, Sun D, He S, Yang F, Yan X, Zhang S, Li N and Chen W: Cancer statistics in China and United States, 2022: Profiles, trends, and determinants. Chin Med J (Engl) 135: 584-590, 2022.
6. Huang H, He Y, Li Y, Gu M, Wu M and Ji L: Eriodictyol suppresses the malignant progression of colorectal cancer by downregulating tissue specific transplantation antigen P35B (TSTA3) expression to restrain fucosylation. Bioengineered 13: 5551-5563, 2022.
7. Schjoldager KT, Narimatsu Y, Joshi HJ and Clausen H: Global view of human protein glycosylation pathways and functions. Nat Rev Mol Cell Biol 21: 729-749, 2020.
8. Costa AF, Campos D, Reis CA and Gomes C: Targeting glycosylation: A new road for cancer drug discovery. Trends Cancer 6: 757-766, 2020.
9. Rini JM, Moremen KW, Davis BG, Esko JD, Varki A, Cummings RD, Esko JD, Stanley P, Hart GW, Aebi M, *et al*: Glycosyltransferases and glycan-processing enzymes. In: Essentials of Glycobiology [Internet]. 4th edition. Cold Spring Harbor Laboratory Press, Cold Spring Harbor, NY, Chapter 47, 2022.
10. Dos Reis JS, da Costa Santos MA, Mendonça DP, do Nascimento SIM, Barcelos PM, de Lima RG, da Costa KM, Freire-de-Lima CG, Morrot A, Previato JO, *et al*: Glycobiology of cancer: Sugar drives the show. Medicines (Basel) 9: 34, 2022.
11. Munkley J and Elliott DJ: Hallmarks of glycosylation in cancer. Oncotarget 7: 35478-35489, 2016.
12. Mereiter S, Balmaña M, Campos D, Gomes J and Reis CA: Glycosylation in the era of cancer-targeted therapy: Where are we heading? Cancer Cell 36: 6-16, 2019.
13. Blanas A, Sahasrabudhe NM, Rodríguez E, van Kooyk Y and van Vliet SJ: Fucosylated antigens in cancer: An alliance toward tumor progression, metastasis, and resistance to chemotherapy. Front Oncol 8: 39, 2018.
14. Gao Z, Wu Z, Han Y, Zhang X, Hao P, Xu M, Huang S, Li S, Xia J, Jiang J and Yang S: Aberrant fucosylation of saliva glycoprotein defining lung adenocarcinomas malignancy. ACS Omega 7: 17894-17906, 2022.
15. Liang JX, Gao W and Cai L: Fucosyltransferase VII promotes proliferation via the EGFR/AKT/mTOR pathway in A549 cells. Onco Targets Ther 10: 3971-3978, 2017.
16. Liu C, Li Z, Wang S, Fan Y, Zhang S, Yang X, Hou K, Tong J, Hu X, Shi X, *et al*: FUT4 is involved in PD-1-related immunosuppression and leads to worse survival in patients with operable lung adenocarcinoma. J Cancer Res Clin Oncol 145: 65-76, 2019.
17. Shah P, Wang X, Yang W, Eshghi ST, Sun S, Hoti N, Chen L, Yang S, Pasay J, Rubin A and Zhang H: Integrated proteomic and glycoproteomic analyses of prostate cancer cells reveal glycoprotein alteration in protein abundance and glycosylation. Mol Cell Proteomics 14: 2753-2763, 2015.
18. Deng G, Chen L, Zhang Y, Fan S, Li W, Lu J and Chen X: Fucosyltransferase 2 induced epithelial-mesenchymal transition via TGF-β/Smad signaling pathway in lung adenocarcinaoma. Exp Cell Res 370: 613-622, 2018.
19. Lai TY, Chen IJ, Lin RJ, Liao GS, Yeo HL, Ho CL, Wu JC, Chang NC, Lee AC and Yu AL: Fucosyltransferase 1 and 2 play pivotal roles in breast cancer cells. Cell Death Discov 5: 74, 2019.
20. Kramer N, Schmöllerl J, Unger C, Nivarthi H, Rudisch A, Unterleuthner D, Scherzer M, Riedl A, Artaker M, Crncec I, *et al*: Autocrine WNT2 signaling in fibroblasts promotes colorectal cancer progression. Oncogene 36: 5460-5472, 2017.
21. Zhan T, Rindtorff N and Boutros M: Wnt signaling in cancer. Oncogene 36: 1461-1473, 2017.
22. Tang Z, Li C, Kang B, Gao G, Li C and Zhang Z: GEPIA: A web server for cancer and normal gene expression profiling and interactive analyses. Nucleic Acids Res 45: W98-W102, 2017.
23. Edge SB and Compton CC: The American joint committee on cancer: The 7th edition of the AJCC cancer staging manual and the future of TNM. Ann Surg Oncol 17: 1471-1474, 2010.
24. Livak KJ and Schmittgen TD: Analysis of relative gene expression data using real-time quantitative PCR and the 2(-Delta Delta C(T)) method. Methods 25: 402-408, 2001.
25. Zhou W, Ma H, Deng G, Tang L, Lu J and Chen X: Clinical significance and biological function of fucosyltransferase 2 in lung adenocarcinoma. Oncotarget 8: 97246-97259, 2017.
26. Mao Y, Zhang Y, Fan S, Chen L, Tang L, Chen X and Lyu J: GALNT6 promotes tumorigenicity and metastasis of breast cancer cell via β-catenin/MUC1-C signaling pathway. Int J Biol Sci 15: 169-182, 2019.
27. Liu J, Xiao Q, Xiao J, Niu C, Li Y, Zhang X, Zhou Z, Shu G and Yin G: Wnt/β-catenin signaling: Function, biological mechanisms, and therapeutic opportunities. Signal Transduct Target Ther 7: 3, 2022.
28. Deschuyter M, Leger DY, Verboom A, Chaunavel A, Maftah A and Petit JM: ST3GAL2 knock-down decreases tumoral character of colorectal cancer cells in vitro and in vivo. Am J Cancer Res 12: 280-302, 2022.
29. Vajaria BN and Patel PS: Glycosylation: A hallmark of cancer? Glycoconj J 34: 147-156, 2017.
30. Tvaroška I: Glycosyltransferases as targets for therapeutic intervention in cancer and inflammation: Molecular modeling insights. Chem Pap 76: 1953-1988, 2022.
31. Vasconcelos-Dos-Santos A, Oliveira IA, Lucena MC, Mantuano NR, Whelan SA, Dias WB and Todeschini AR: Biosynthetic machinery involved in aberrant glycosylation: Promising targets for developing of drugs against cancer. Front Oncol 5: 138, 2015.
32. Liang Y, Wang T, Gao R, Jia X, Ji T, Shi P, Xue J, Yang A, Chen M and Han P: Fucosyltransferase 8 is overexpressed and influences clinical outcomes in lung adenocarcinoma patients. Pathol Oncol Res 28: 1610116, 2022.

33. Blanas A, Zaal A, van der HaarÀvila I, Kempers M, Kruijssen L, de Kok M, Popovic MA, van der Horst JC and van Vliet SJ: FUT9-driven programming of colon cancer cells towards a stem cell-like state. Cancers (Basel) 12: 2580, 2020.
34. Stewart ZA, Westfall MD and Pietenpol JA: Cell-cycle dysregulation and anticancer therapy. Trends Pharmacol Sci 24: 139-145, 2003.
35. Tang H, Yang P, Yang X, Peng S, Hu X and Bao G: Growth factor receptor bound protein-7 regulates proliferation, cell cycle, and mitochondrial apoptosis of thyroid cancer cells via MAPK/ERK signaling. Mol Cell Biochem 472: 209-218, 2020.
36. Hiremath IS, Goel A, Warrier S, Kumar AP, Sethi G and Garg M: The multidimensional role of the Wnt/β-catenin signaling pathway in human malignancies. J Cell Physiol 237: 199-238, 2022.
37. Cebrat M, Strzadala L and Kisielow P: Wnt inhibitory factor-1: A candidate for a new player in tumorigenesis of intestinal epithelial cells. Cancer Lett 206: 107-113, 2004.
38. Huang HL, Tang GD, Liang ZH, Qin MB, Wang XM, Chang RJ and Qin HP: Role of Wnt/β-catenin pathway agonist SKL2001 in Caerulein-induced acute pancreatitis. Can J Physiol Pharmacol 97: 15-22, 2019.
39. Shang S, Hua F and Hu ZW: The regulation of β-catenin activity and function in cancer: Therapeutic opportunities. Oncotarget 8: 33972-33989, 2017.
40. Stamos JL and Weis WI: The β-catenin destruction complex. Cold Spring Harb Perspect Biol 5: a007898, 2013.
41. Jung YS, Jun S, Lee SH, Sharma A and Park JI: Wnt2 complements Wnt/β-catenin signaling in colorectal cancer. Oncotarget 6: 37257-37268, 2015.
42. Huang C, Ma R, Xu Y, Li N, Li Z, Yue J, Li H, Guo Y and Qi D: Wnt2 promotes non-small cell lung cancer progression by activating WNT/β-catenin pathway. Am J Cancer Res 5: 1032-1046, 2015.
43. Rahiminejad S, Maurya MR, Mukund K and Subramaniam S: Modular and mechanistic changes across stages of colorectal cancer. BMC Cancer 22: 436, 2022.